

Supporting Information

Inorganic-organic Hybridization Induced Uniaxial Zero Thermal Expansion in MC_4O_4 (M = Ba, Pb)

Zhanning Liu,^a Kun Lin,^a Yang Ren,^b Kenichi Kato,^c Yili Cao,^a Jinxia Deng,^a Jun Chen,^a and
Xianran Xing^{*a}

- Beijing Advanced Innovation Center for Materials Genome Engineering, Department of Physical Chemistry, University of Science and Technology Beijing, Beijing, 100083, China
- X-Ray Science Division, Argonne National Laboratory, Argonne, Illinois 60439, United States.
- RIKEN SPring-8 Center, Hyogo 679-5148, Japan

1. Materials and detail of synthesis

All of the chemicals used in this experiment were analytical grade and used without further purification.

BaC₄O₄: Squaric acid (114mg, 1 mmol), NaOH (80 mg, 2 mmol) and Ba(NO₃)₂ (261mg, 1 mmol) were dissolved in 20 ml deionized water under stirring. Then the mixture was transferred into a 50 ml Teflon-lined autoclave and heated at 80 °C for 48h. After cooling to room temperature, colorless crystals were collected.

PbC₄O₄: Squaric acid (456mg, 4 mmol), and Pb(NO₃)₂ (331mg, 1 mmol) were dissolved in 25 ml deionized water under stirring. Then the mixture was transferred into a 50 ml Teflon-lined autoclave and heated at 180 °C for 24h. After cooling to room temperature, white powder products were collected.

Before measurements, all samples were washed several times with deionized water and ethanol, and dried at 120 °C overnight.

2. Laboratory powder X-ray diffraction

The laboratory powder X-ray diffraction (PXRD) data were collected on a PANalytical diffractometer with Cu K α radiation.

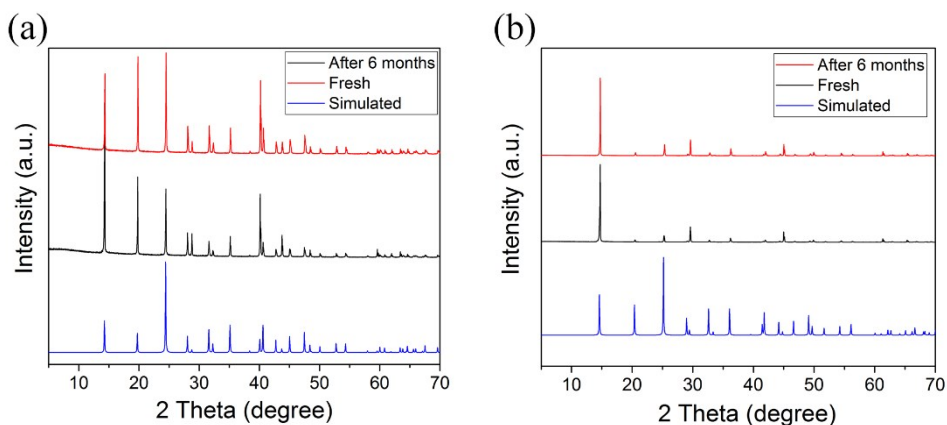


Figure S1 (a) PXRD patterns of the simulated BaC_4O_4 (blue), freshly synthesized BaC_4O_4 (black) and the one exposed in air for 6 months (red). (b) PXRD patterns of the simulated PbC_4O_4 (blue), freshly synthesized PbC_4O_4 (black) and the one exposed in air for 6 months (red).

3. Thermo-gravimetric analysis

Thermo Gravimetric-Differential Scanning Calorimetry (TG-DSC) measurement was performed using a Labsys Evo system (by SETRAM) with a rate of $5^\circ\text{C}\cdot\text{min}^{-1}$ under air.

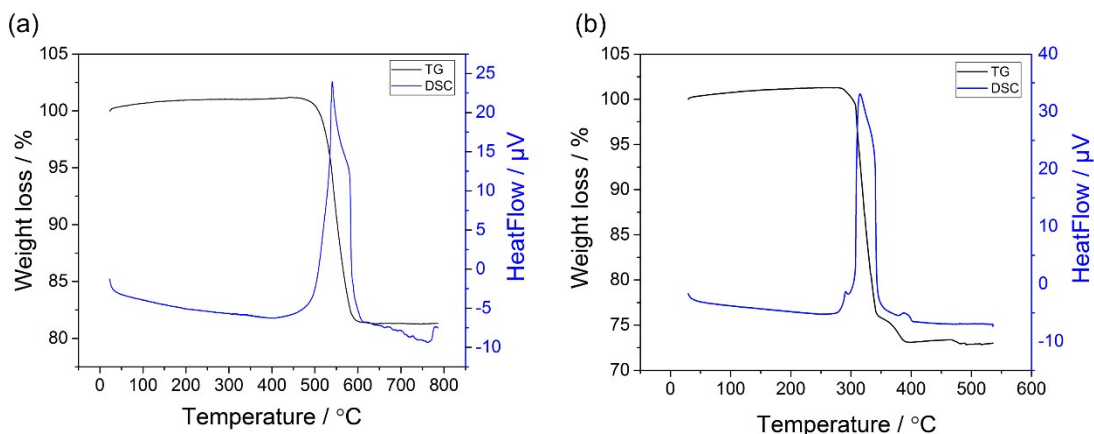


Figure S2. TG-DSC curves of BaC_4O_4 (a) and PbC_4O_4 (b). The weight loss and the exothermic peak at 500°C (a) and 300°C (b) corresponds to the decomposition of the compound.

4. Variable temperature synchrotron X-ray diffraction

Variable temperature synchrotron X-ray diffraction (SXRD) were collected at the SPring-8 BL44B2 beamline for BaC_4O_4 and PbC_4O_4 . Before loading, both samples are grinded into powder. Then, the powder samples are loaded into 0.5 mm capillaries and sealed in air. The wavelength was calibrated

to $\lambda = 0.45 \text{ \AA}$ using a CeO_2 standard. The data were collected from 125 K to 700 K (125 to 550 K for PbC_4O_4) with a heating rate 50 K min^{-1} .

The variable temperature SXR D data were analyzed by Rietveld refinement using the Fullprof program^[1] (Figure S3). The background was modelled by a 6-coefficients polynomial function. The scale factor, lattice parameters, zero point were also refined. The Pseudo-voigt function was chosen to generate the peak shapes. The coordinates and isotropic atomic displacement parameter were refined for all atoms. The result of the final Rietveld refinement plot and results are shown in figure S3, Table S1 and Table S2. The lattice parameters extracted from Rietveld refinements are listed in Table S3 and S4.

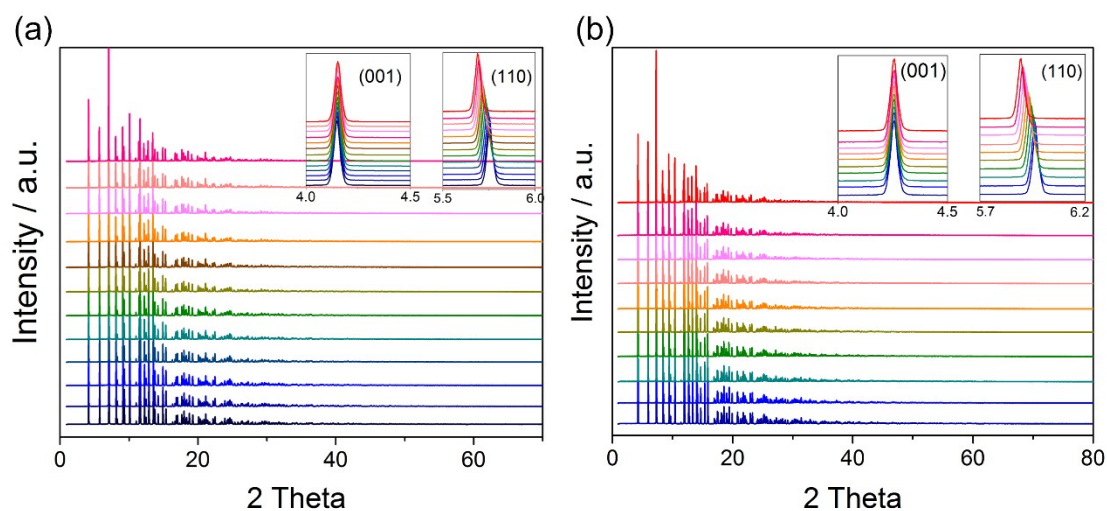


Figure S3. Temperature dependent synchrotron X-ray diffraction patterns of BaC_4O_4 (a) and PbC_4O_4 (b). The insets are the zoomed peaks of (001) and (110). From bottom to top correspond to the temperature 125, 150, 200, 250, 300, 350, 400, 450, 500, 550, 600, 650, 700 K (550K for PbC_4O_4).

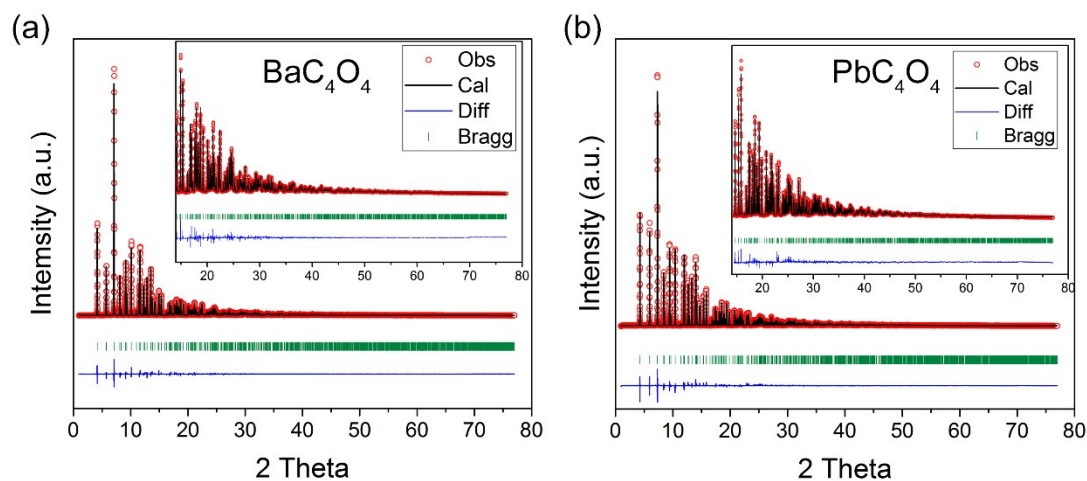


Figure S4 Rietveld refinement of SXR D data of BaC_4O_4 (a) and PbC_4O_4 (b) at 300 K. Zoomed in parts at high angles are shown in the inset. ($R_p=8.46$, $R_{wp}=9.88$, $\chi^2=10.00$ for BaC_4O_4 , and $R_p=9.99$, $R_{wp}=10.8$, $\chi^2=7.42$ for PbC_4O_4).

Table S1 Atomic coordinates, thermal parameters and occupancy for BaC₄O₄ extracted from the Rietveld refinement.

Atom	x	y	z	Occupancy	Uiso	Multiplicity & Wyckoff
Ba	0.0000	0.0000	0.2500	1.000	0.004	4a
O	0.1789	0.3210	0.1330	1.000	0.006	16l
C	0.0817	0.4183	0.0589	1.000	0.004	16l

Table S2 Atomic coordinates, thermal parameters and occupancy for PbC₄O₄ extracted from the Rietveld refinement.

Atom	x	y	z	Occupancy	Uiso	Multiplicity & Wyckoff
Pb	0.0000	0.0000	0.2500	1.000	0.004	4a
O	0.1852	0.3148	0.1353	1.000	0.007	16l
C	0.0867	0.4133	0.0581	1.000	0.001	16l

Table S3 Temperature dependent lattice parameters of BaC₄O₄ derived from the Rietveld refinement

Temperature / K	<i>a</i> / Å	<i>c</i> / Å	<i>V</i> / Å ³
125	6.3327(3)	12.4103(6)	497.687(7)
150	6.3356(3)	12.4091(6)	498.093(7)
200	6.3415(3)	12.4071(5)	498.949(7)
250	6.3478(4)	12.4052(5)	499.862(7)
300	6.3543(4)	12.4033(5)	500.803(7)
350	6.3606(4)	12.4019(5)	501.742(7)
400	6.3668(4)	12.4005(6)	502.667(8)
450	6.3730(4)	12.3993(6)	503.606(8)
500	6.3794(4)	12.3980(6)	504.559(8)
550	6.3860(4)	12.3966(7)	505.546(8)
600	6.3922(5)	12.3957(7)	506.488(8)
650	6.3984(5)	12.3951(7)	507.451(8)
700	6.4050(5)	12.3945(7)	508.469(8)

Table S4 Temperature dependent lattice parameters of PbC₄O₄ derived from the Rietveld refinement

Temperature / K	<i>a</i> / Å	<i>c</i> / Å	<i>V</i> / Å ³
125	6.1089(3)	12.0941(5)	451.342(7)
150	6.1128(3)	12.0941(5)	451.909(7)
200	6.1208(3)	12.0938(5)	453.080(7)
250	6.1291(3)	12.0936(5)	454.305(7)
300	6.1376(4)	12.0931(6)	455.545(7)
350	6.1460(4)	12.0928(6)	456.785(8)

400	6.1541(4)	12.0925(6)	457.979(8)
450	6.1623(4)	12.0921(6)	459.191(8)
500	6.1709(5)	12.0917(7)	460.452(8)
550	6.1802(5)	12.0910(7)	461.809(8)

Table S5 Some reported inorganic-organic hybrid materials with ZTE behavior.

Compound	CTE ($\times 10^{-6}$ K ⁻¹)	Temperature range (K)	Reference
NiPt(CN) ₆	$\alpha_a = -1.02$	100~330	<i>JACS</i> , 2006, 128, 7009-7014. ^[2]
Fe[Co(CN) ₆]	$\alpha_a = -1.47$	4.2~300	<i>JACS</i> , 2004, 126, 15390-15391. ^[3]
(C ₃ H ₅ N ₂) ₂ K[Co(CN) ₆]	$\alpha_a = +1.7$	200~300	<i>Angew. Chem.</i> 2017, 129, 16166-16169. ^[4]
[Cd(HBTC)(BPP)]·1.5DMF·2H ₂ O	$\alpha_{x2} = +2$	100~260	<i>Chem. Comm.</i> 2014, 50, 6464-6467. ^[5]
N(CH ₃) ₄ CuZn(CN) ₄	$\alpha_a = +0.67$	218~368	<i>JACS</i> , 2010, 132, 10-11. ^[6]
ZnTe(N ₂ H ₄) _{0.5}	$\alpha_a = +3.759$	95~295	<i>JACS</i> , 2007, 129, 14140-14141. ^[7]
β -ZnTe(en) _{0.5}	$\alpha_b = \sim +0.43$	4~400	<i>PRL</i> , 99, 215901, 2007. ^[8]

5. Variable temperature synchrotron X-ray pair distribution function

The pair distribution function (PDF) data were extracted from high energy synchrotron X-ray scattering by direct Fourier transform of reduced structure function (F(Q), up to Q = 22 Å⁻¹) using the 11-ID-C beamline at Advanced Photon Source (APS) of Argonne National Laboratory. The PDF profile refinements were carried out for BaC₄O₄ and PbC₄O₄ using PDFgui program.^[9] The parameters, including lattice constants, atomic position, and anisotropic thermal ellipsoids, are allowed to vary until a best-fit of the PDF is obtained, using a least-squares approach.

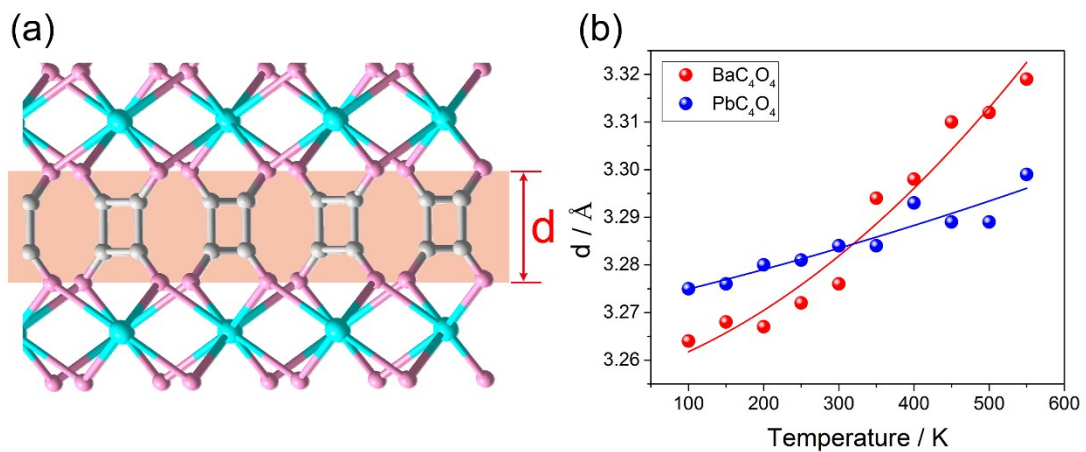


Figure S5 (a) Crystal structure of BaC_4O_4 . (b) Thermal expansion behavior of the squarate pillar along c axis (distance between two oxygen atoms along c axis) for BaC_4O_4 (red) and PbC_4O_4 (blue).

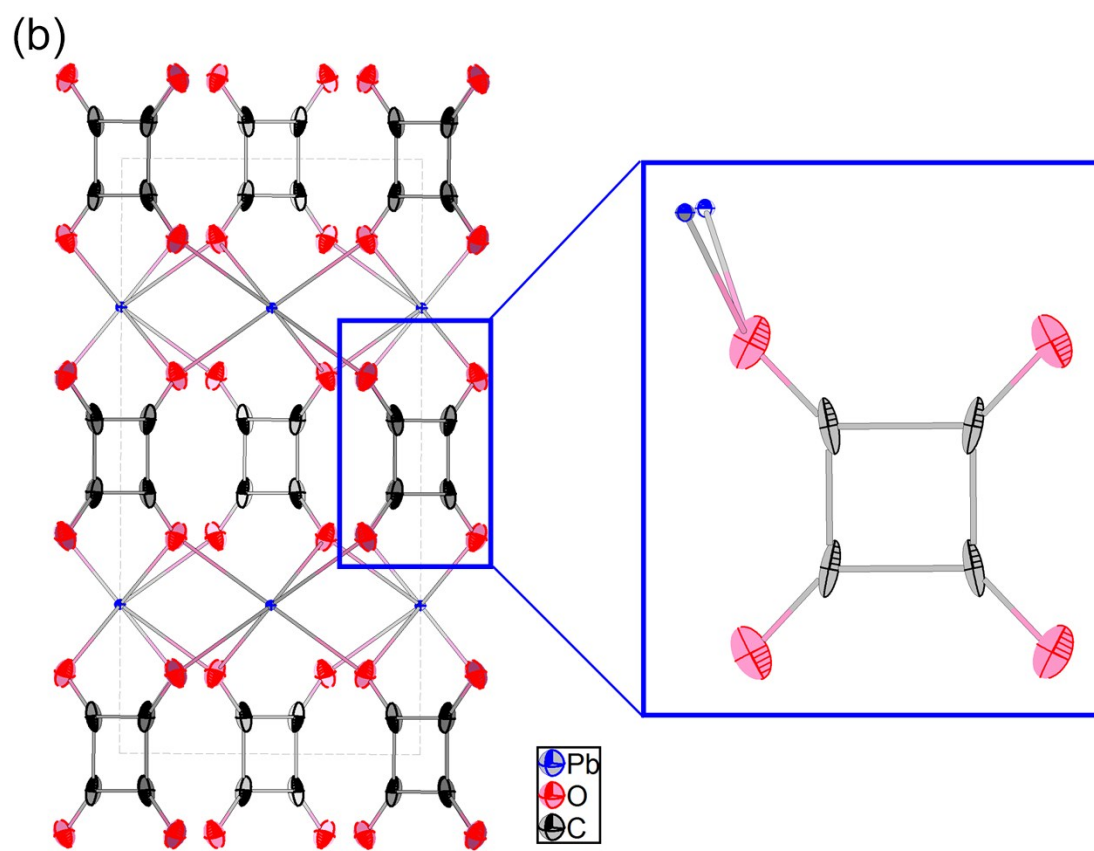
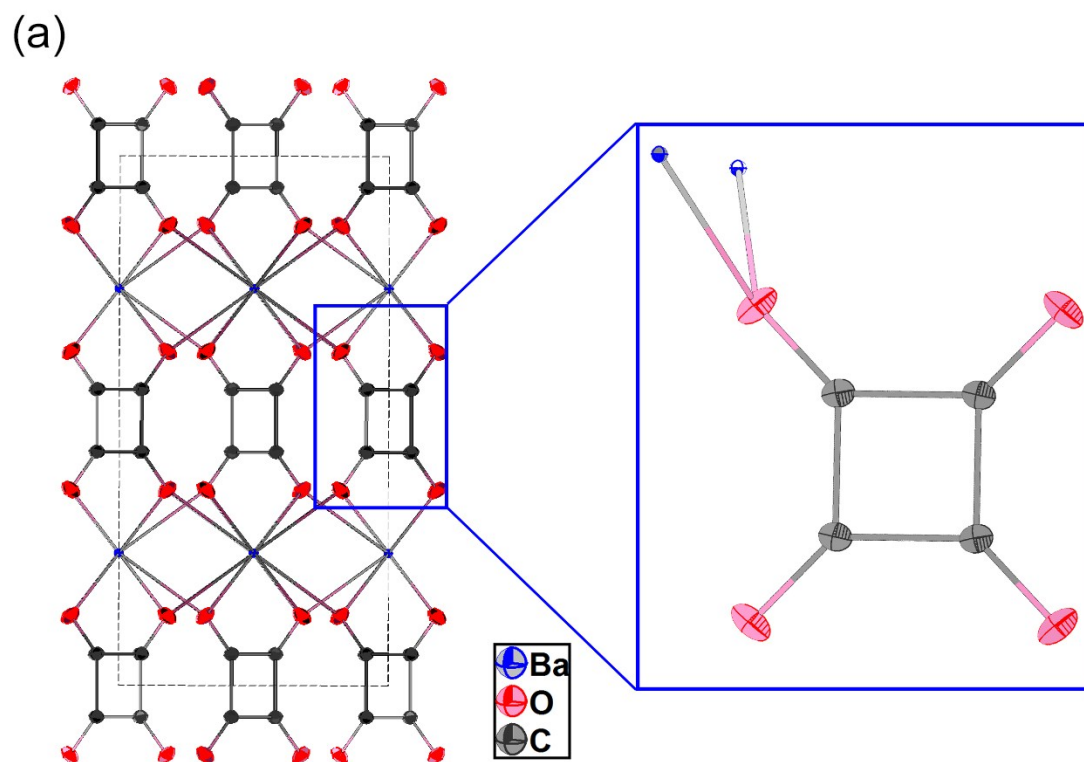


Figure S6. Thermal ellipsoid plot of BaC_4O_4 (a) and PbC_4O_4 (b) derived from the PDF fitting (drawn at 50% probability). Color code: blue for barium or lead, red for oxygen, gray for carbon.

6. Variable temperature Raman spectra and DFT calculation

The variable temperature Raman measurements were performed with a multichannel modular triple Raman system (JY-HR800) with confocal microscopy. The spot diameter of the focused laser beam on the sample is about 1 μm . The solid-state diode laser (532nm) from Coherent Company-Verdi-2 was used as an excited source. Sample temperature was controlled by a temperature-controlled stage (Linkam) from 100 to 600 K with an interval of 100 K for BaC_4O_4 (100 to 500 K with an interval of 50 K for PbC_4O_4).

The first-principles atomic vibration modes assignment was performed by the plane-wave pseudopotential density functional theory (DFT)^[10] implemented by CASTEP package.^[11] The generalized gradient approximation (GGA) with Perdew–Burke–Ernzerhof (PBE)^[12] functional was adopted and the ion-electron interactions were modeled by the optimized normal-conserving pseudopotentials^[13] for all elements. The kinetic energy cutoffs of 800 eV and Monkhorst-Pack^[14] k-point meshes with the spanning grid less than $0.04/\text{\AA}^3$ in the Brillouin zone were chosen. Before the atomic vibration calculation, the crystal structure was fully optimized by Broyden–Fletcher–Goldfarb–Shanno (BFGS)^[15] minimization scheme with the convergence criterions for energy, maximum force, maximum stress and maximum displacement set as 10^{-5} eV/atom, 0.03 eV, 0.05 GPa and 0.001 \AA respectively. The vibrational property was calculated by linear response formalism,^[16] in which the phonon frequencies were obtained by the second derivative of the total energy with respect to the given perturbation.^[17]

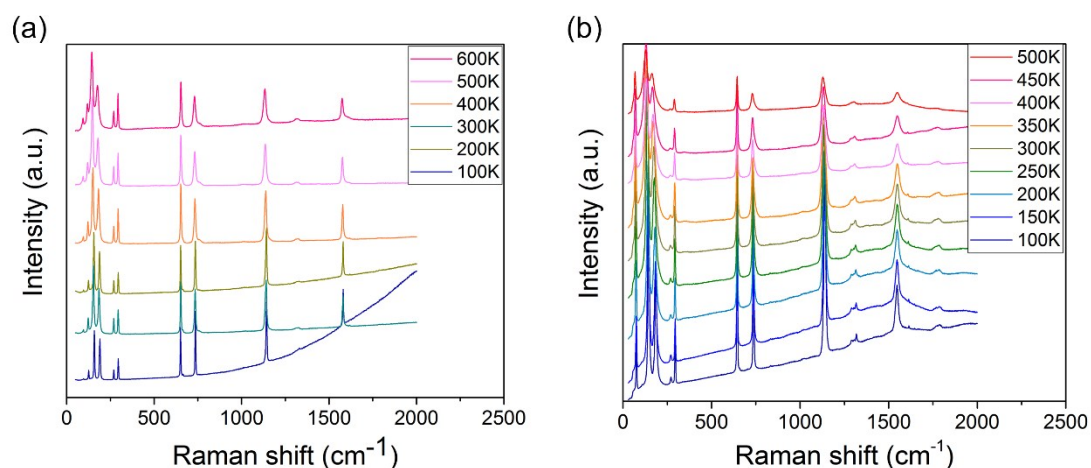


Figure S7 Temperature dependent Raman spectra of BaC_4O_4 (a) and PbC_4O_4 (b).

Table S6 Temperature dependent Raman modes of BaC_4O_4 (some weak peaks are omitted.)

Temperature / K	Mode1	Mode2	Mode3	Mode4	Mode5	Mode6	Mode7	Mode8	Mode9	Mode10
100	96.45	125.67	158.305	189.97	269.50	295.06	651.15	735.99	1143.3	1580.8
200	96.36	124.60	155.88	188.09	269.40	294.66	651.69	735.52	1141.9	1579.94
300	95.70	123.16	152.83	185.07	269.28	294.38	652.22	734.63	1139.9	1579.23
400	95.23	121.43	149.46	182.07	268.75	294.20	652.79	733.36	1138.1	1578.21

									5	
500	94.72	119.51	147.04	178.73	268.72	294.00	652.88	732.17	1135.7	1576.55
									2	
600	93.71	118.85	143.54	176.15	268.71	293.53	653.17	731.22	1133.4	1574.77

Table S7 Temperature dependent Raman modes of PbC₄O₄ (some weak perks are omitted.)

Temperature / K	Mode1	Mode2	Mode3	Mode4	Mode5	Mode6	Mode7	Mode8	Mode9	Mode10
100	76.26	108.31	145.80	185.99	271.48	295.03	644.96	737.09	1139.2	1547.85
									9	
150	74.99	106.88	143.73	183.71	270.71	294.75	644.85	736.18	1138.0	1547.73
									2	
200	74.08	105.11	141.30	180.00	269.84	293.74	644.93	735.30	1136.9	1547.66
									7	
250	73.08	103.09	138.46	176.33	269.33	293.23	644.88	734.36	1135.2	1547.64
									9	
300	71.96	101.24	136.09	173.98	268.26	292.73	644.94	733.67	1134.5	1547.38
									9	
350	71.03	99.86	133.38	170.90	267.80	291.96	644.77	732.50	1132.7	1547.06
									2	
400	70.04	96.48	132.22	169.51	267.18	291.22	644.32	732.05	1131.5	1547.06
									8	
450	69.38	93.50	130.08	166.88	266.85	291.11	644.66	731.76	1130.8	1546.70
									6	
500	68.69	92.87	127.09	164.31	266.45	290.73	644.25	729.91	1128.6	1546.39
									3	

Reference:

- [1] J. Rodriguez-Carvajal, in *satellite meeting on powder diffraction of the XV congress of the IUCr, Vol. 127*, Toulouse, France:[sn], **1990**.
- [2] K. W. Chapman, P. J. Chupas, C. J. Kepert, *Journal of the American Chemical Society* **2006**, *128*, 7009-7014.
- [3] S. Margadonna, K. Prassides, A. N. Fitch, *Journal of the American Chemical Society* **2004**, *126*, 15390-15391.
- [4] A. E. Phillips, A. D. Fortes, *Angewandte Chemie* **2017**, *129*, 16166-16169.
- [5] P. Lama, R. K. Das, V. J. Smith, L. J. Barbour, *Chemical Communications* **2014**, *50*, 6464-6467.
- [6] A. E. Phillips, G. J. Halder, K. W. Chapman, A. L. Goodwin, C. J. Kepert, *Journal of the American Chemical Society* **2009**, *132*, 10-11.
- [7] J. Li, W. Bi, W. Ki, X. Huang, S. Reddy, *Journal of the American Chemical Society* **2007**, *129*, 14140-14141.
- [8] Y. Zhang, Z. Islam, Y. Ren, P. Parilla, S. Ahrenkiel, P. Lee, A. Mascarenhas, M. McNevin, I. Naumov, H.-X. Fu, *Physical review letters* **2007**, *99*, 215901.

- [9] C. Farrow, P. Juhas, J. Liu, D. Bryndin, E. Božin, J. Bloch, T. Proffen, S. Billinge, *Journal of Physics: Condensed Matter* **2007**, *19*, 335219.
- [10] M. C. Payne, M. P. Teter, D. C. Allan, T. Arias, a. J. Joannopoulos, *Reviews of modern physics* **1992**, *64*, 1045.
- [11] S. J. Clark, M. D. Segall, C. J. Pickard, P. J. Hasnip, M. I. Probert, K. Refson, M. C. Payne, *Zeitschrift für Kristallographie-Crystalline Materials* **2005**, *220*, 567-570.
- [12] J. P. Perdew, K. Burke, M. Ernzerhof, *Phys. Rev. Lett* **1996**, *77*, 3865-3868.
- [13] D. Hamann, M. Schlüter, C. Chiang, *Physical Review Letters* **1979**, *43*, 1494.
- [14] H. Monkshort, J. Pack, *Phys. Rev. B* **1976**, *13*, 5188-5192.
- [15] B. G. Pfrommer, M. Côté, S. G. Louie, M. L. Cohen, *Journal of Computational Physics* **1997**, *131*, 233-240.
- [16] S. Baroni, S. De Gironcoli, A. Dal Corso, P. Giannozzi, *Reviews of Modern Physics* **2001**, *73*, 515.
- [17] V. Deyirmenjian, V. Heine, M. Payne, V. Milman, R. Lynden-Bell, M. Finnis, *Physical Review B* **1995**, *52*, 15191.